ISSN: 2158-284X Volume 12, Number 7, July 2021

Scientific Research Publishing

International Journal of Clinical Medicine

ISSN: 2158-284X
9 772158 284007 07

https://www.scirp.org/journal/ijcm

Journal Editorial Board

ISSN: 2158-284X (Print) ISSN: 2158-2882 (Online)
https://www.scirp.org/journal/ijcm

International Journal of Clinical Medicine, 2021, 12, 273-305
https://www.scirp.org/journal/ijcm
ISSN Online: 2158-2882
ISSN Print: 2158-284X

Table of Contents

Volume 12 Number 7 July 2021

International Journal of Clinical Medicine (IJCM)
Journal Information

SUBSCRIPTIONS

The *International Journal of Clinical Medicine* (Online at Scientific Research Publishing, https://www.scirp.org/) is published monthly by Scientific Research Publishing, Inc., USA.

Subscription rates:
Print: $79 per issue.
To subscribe, please contact Journals Subscriptions Department, E-mail: sub@scirp.org

SERVICES

Advertisements
Advertisement Sales Department, E-mail: service@scirp.org

Reprints (minimum quantity 100 copies)
Reprints Co-ordinator, Scientific Research Publishing, Inc., USA.
E-mail: sub@scirp.org

COPYRIGHT

PRODUCTION INFORMATION

For manuscripts that have been accepted for publication, please contact:
E-mail: ijcm@scirp.org

International Journal of Clinical Medicine, 2021, 12, 273-278
https://www.scirp.org/journal/ijcm
ISSN Online: 2158-2882
ISSN Print: 2158-284X

Venovenous ECMO in Severe ARDS

Fouzia Douirek[1], Nada Samkaoui[2], Manal Rhezali[1], Mohamed Abdenasser Samkaoui[1]

[1]Polyvalent Intensive Care Unit, Arrazi Hospital, Mohammed VI[th] University Centre, Cadi Ayyad University, Marrakech, Morocco
[2]Medical University of Warsaw, Warszawa, Poland
Email: fouzia-douirek@hotmail.fr

How to cite this paper: Douirek, F., Samkaoui, N., Rhezali, M. and Samkaoui, M.A. (2021) Venovenous ECMO in Severe ARDS. *International Journal of Clinical Medicine*, **12**, 273-278.
https://doi.org/10.4236/ijcm.2021.127024

Received: May 2, 2021
Accepted: July 4, 2021
Published: July 7, 2021

Abstract

The Veno-venous Extra Corporeal Membrane Oxygenation (ECMO) indications and usage has strikingly progressed over the last years; especially with the COVID 19 pandemic, it has become an essential tool in the care of adults and children with severe pulmonary dysfunction refractory to conventional management. In this article, we will provide a review of ECMO development, clinical indications, patients' management, options and cannulations techniques, complications, outcomes, and the appropriate strategy of organ management while on ECMO.

Keywords

Critical Care, Extracorporeal Membrane Oxygenation, Intensive Care Units, Respiratory Distress Syndrome, Respiratory Failure, Review, Ventilation Artificial

1. Introduction

Acute Respiratory Distress Syndrome (ARDS) is a severe pulmonary and systemic disease with a high mortality rate, especially in the most severe forms with refractory hypoxemia. Despite the use of exceptional adjunctive therapies, mortality exceeds 60% [1]. This has motivated some teams to use an extracorporeal circuit combining a centrifugal pump and a membrane oxygenator, providing total pulmonary assistance allowing blood oxygenation and CO_2 extraction, this technique is also called ECMO for Extra Corporeal Membrane Oxygenation [2]. This review is a practical summary of VV ECMO.

2. ARDS Definition

The most common indication for ECMO in respiratory failure is severe ARDS, which is basically defined by the presence of bilateral infiltrates on chest imaging

within 7 days of an inciting event and impaired oxygenation (PaO_2/FIO_2 ratio < 100 mm Hg while receiving positive-pressure ventilation), which is not fully explained by cardiogenic pulmonary edema [3].

The acute respiratory distress syndrome (ARDS) was defined in 1994 by the American-European Consensus Conference (AECC); since then, issues regarding the reliability and validity of this definition have emerged. Using a consensus process, a panel of experts convened in 2011 and developed the *Berlin Definition*, composed of 3 mutually exclusive categories of ARDS based on degree of hypoxemia: mild ($PaO_2/FIO_2 \leq 300$ mm Hg), moderate ($PaO_2/FIO_2 \leq 200$ mm Hg), and severe ($PaO_2/FIO_2 \leq 100$ mm Hg) [3].

ARDS is an acute, diffuse, inflammatory lung injury that leads to increased pulmonary vascular permeability, pulmonary compliance reduction, ventilation/perfusion mismatch, consolidation and alveolar collapses, surfactant defect and systemic repercussions via inflammatory cytokine release.

The standard of care for invasive mechanical ventilation in ARDS is a volume- and pressure-limited ventilation strategy, which improves survival, in large part through the minimization of ventilator-associated lung injury (VALI).

3. ECMO

ECMO stands for a circulatory and/or ventilatory assistance technique allowing respiratory or cardiac support while the underlying pathology is reversed or resolved. There are two main types of ECMO: venous (VV) and venous arterial (VA), they each have precise indications, advantages but also common and specific complications.

It requires a specific and specialized environment with trained staff capable of managing its associated difficulties and possible complications.

4. Physiology

ECMO refers to a circuit that directly oxygenates and removes carbon dioxide from blood through an extracorporeal gas exchange device, commonly referred to as a membrane oxygenator. The oxygenator consists of a semipermeable membrane that separates a blood compartment from a gas compartment, allowing only gas molecules to diffuse between compartments.

At the time of ECMO initiation, catheters (or cannulas) are placed in central vessels. Deoxygenated blood is drained from the body by an external pump, after which it passes through the membrane oxygenator and is reinfused back into the patient. When the drainage and reinfusion cannulas are both located in central veins, the circuit is referred to as venovenous ECMO, and the device provides gas exchange support only. When blood is drained from a vein and reinfused into an artery, it is referred to as venoarterial ECMO, and the circuit provides both gas exchange and circulatory support [4].

Typically, venovenous ECMO is used for respiratory failure such as ARDS whereas veno-arterial ECMO is indicated in cases with respiratory and hemo-

dynamic instability.

5. Indications for Venovenous ECMO

The most common indication for ECMO in respiratory failure is severe ARDS. It is also the only indication with a high level of evidence through randomized controlled studies. Other potential indications based only on cohort studies include: acute hypercapnic respiratory failure, a bridge to lung transplantation or as a primary graft dysfunction after lung transplantation, or in case of pulmonary hypertension with right ventricular failure [4].

In all cases, ECMO is considered as a temporary solution biding for recovery of the underlying condition or for a lung transplant [5].

6. Contraindications

Relative contraindications to ECMO in acute respiratory failure include the prolonged use of high-pressure ventilation or high FIO_2, limited vascular access, contraindications to the use of anticoagulation, and the presence of any condition or organ dysfunction that would limit the likelihood of overall benefit from ECMO (eg, severe irreversible brain injury or untreatable metastatic cancer). An absolute contraindication to ECMO is the presence of severe irreversible respiratory failure if transplantation will not be considered.

The assessment process can be based on progonostic scoring systems that help risk stratify patients being considered for ECMO in respiratory failure [6].

The decision to implant ECMO requires careful assessment of the risk-benefit balance. The contraindications must be respected insofar as these patients can no longer live without ECMO with a highly improbable recovery and are not candidates for definitive therapy, which constitutes for a real ethical dilemma [7].

7. Complications

ECMO is an invasive therapy associated with multiple complications, ranging from hemorrhage to thromboembolic events and an increased risk of infection [8] [9]. This implies the need for continuous systemic anticoagulation to maintain ECMO circuit patency and minimize the risk of thrombosis in both the circuit and the patient; this requires a strict balance control of both thrombotic risk and the potential hemorrhagic complications [10].

Hematological disorders are also very commonly associated to ECMO practice, including hemolysis, thrombocytopenia, acquired Von Willebrand syndrome and disseminated intravascular coagulopathy [4] [11].

8. Evidence for ECMO Use as a Treatment Line in ARDS

ECMO has been developed as a second line management therapy for severe ARDS cases, and has recently been the object of randomized controlled trials to establish its efficacy and safety.

Many Cohort series demonstrated a high survival rate in patients with severe ARDS using ECMO and pressure-supported ventilation with minimal sedation [12] [13].

The results of the EOLIA trial were published in 2018 involving patients with very severe forms of ARDS defined by a PaO_2/FiO_2 ratio of less than 50 mmHg for more than 3 hours or less than 80 mmHg for more than 6 hours or respiratory acidosis with a pH < 7.25 and a $paCO_2$ > 60 mmhg for more than 6 hours. Patients were randomized to receive either conventional treatment (control group) or immediate venous-venous ECMO. Cross-over to ECMO was possible for patients in the control group who had refractory hypoxemia. The primary endpoint was 60-day mortality.

Among the very severe ARDS patients in the EOLIA study, the 60-day mortality was not significantly lower with the use of ECMO as a rescue treatment compared to a conventional ventilatory strategy. In addition, the rate of hemorrhagic or ischemic complications was similar between the two groups [14].

However, a post-hoc Bayesian analysis of the EOLIA data showed a high likelihood of survival benefit with ECMO under a broad set of assumptions [15].

A recently published meta-analysis suggests that the use of venovenous ECMO in adults with severe acute respiratory distress syndrome was associated with reduced 60-day mortality compared with conventional mechanical ventilation. However, venovenous ECMO was also associated with a moderate risk of major bleeding [16].

The role of ECMO in the most severe forms of ARDS is evolving. It is not a substitute for lung-protective ventilation and adherence to other proven strategies, when such strategies are available and applied appropriately. Likewise, the use of algorithm based treatments and selection of patients suitable for ECMO therapy is a must as it should not be considered as a first-line therapy for ARDS rather than a justified decision under specific circumstances when the current standard of care is insufficient to support the patient [17].

9. Prognosis

Few large scale studies have evaluated long term quality recovery of survival patients after severe ARDS who benefited from ECMO assistance. A follow-up program including twenty-one long term survivors showed that the majority of patients had good physical and social functioning but a reduced health related quality of life according to the St George's Respiratory Questionnaire (SGRQ). Lung parenchymal changes on high-resolution computed tomography were suggestive of fibrosis and minor pulmonary function abnormalities remained common and can be detected more than 1 year after ECMO [18].

10. Conclusion

ECMO is an assistance technique capable of supporting severe hematosis disorders in acute respiratory failure, with data showing potential benefits for im-

proving survival in patients with severe ARDS. Its use should remain in centers sufficiently experienced with the procedure in specific indications as additional research is needed before ECMO can be recommended for more extensive practice.

Funding Source

This research did not receive any specific grant from funding agencies in the public, commercial, or not-for-profit sectors.

Conflicts of Interest

The authors declare no conflicts of interest regarding the publication of this paper.

References

[1] Bellani, G., Laffey, J.G., Pham, T., Fan, E., Brochard, L., Esteban, A., *et al.* (2016) Epidemiology, Patterns of Care, and Mortality for Patients with Acute Respiratory Distress Syndrome in Intensive Care Units in 50 Countries. *The Journal of the American Medical Association*, **315**, 788-800. https://doi.org/10.1001/jama.2016.0291

[2] Brodie, D. and Bacchetta, M. (2011) Extracorporeal Membrane Oxygenation for ARDS in Adults. *The New England Journal of Medicine*, **365**, 1905-1914. https://doi.org/10.1056/NEJMct1103720

[3] Ranieri, V.M., Rubenfeld, G.D., Thompson, B.T., Ferguson, N.D., Caldwell, E., *et al.* (2012) ARDS Definition Task Force, Acute Respiratory Distress Syndrome: The Berlin Definition. *The Journal of the American Medical Association*, **307**, 2526-2533.

[4] Abrams, D. and Brodie, D. (2017) Extracorporeal Membrane Oxygenation for Adult Respiratory Failure: 2017 Update. *Chest*, **152**, 639-649. https://doi.org/10.1016/j.chest.2017.06.016

[5] Richard, C., Argaud, L., Blet, A., Boulain, T., Contentin, L., *et al.* (2014) Extracorporeal Life Support for Patients with Acute Respiratory Distress Syndrome: Report of a Consensus Conference. *Annals of Intensive Care*, **4**, 15. https://www.ncbi.nlm.nih.gov/pmc/articles/PMC4046033/

[6] Schmidt, M., Zogheib, E., Rozé, H., Repesse, X., Lebreton, G., Luyt, C.-E., *et al.* (2013) The Preserve Mortality Risk Score and Analysis of Long-Term Outcomes after Extracorporeal Membrane Oxygenation for Severe Acute Respiratory Distress Syndrome. *Intensive Care Medicine*, **39**, 1704-1713. https://doi.org/10.1007/s00134-013-3037-2

[7] Mosier, J.M., Kelsey, M., Raz, Y., Gunnerson, K.J., Meyer, R., Hypes, C.D., Malo, J., Whitmore, S.P. and Spaite, D.W. (2015) Extracorporeal Membrane Oxygenation (ECMO) for Critically Ill Adults in the Emergency Department: History, Current Applications, and Future Directions. *Crit Care*, **19**, 431. https://pubmed.ncbi.nlm.nih.gov/26672979/

[8] Schmidt, M., Bréchot, N., Hariri, S., Guiguet, M., Luyt, C.E., Makri, R., *et al.* (2012) Nosocomial Infections in Adult Cardiogenic Shock Patients Supported by Venoarterial Extracorporeal Membrane Oxygenation. *Clinical Infectious Diseases*, **55**, 1633-1641. https://doi.org/10.1093/cid/cis783

[9] Paden, M.L., Rycus, P.T. and Thiagarajan, R.R. (2014) Update and Outcomes in

Extracorporeal Life Support. *Seminars in Perinatology*, **38**, 65-70. https://doi.org/10.1053/j.semperi.2013.11.002

[10] Eric, S., Sklar, M.C., Lequier, L., Fan, E. and Kanji, H.D. (2017) Anticoagulation Practices and the Prevalence of Major Bleeding, Thromboembolic Events, and Mortality in Venoarterial Extracorporeal Membrane Oxygenation: A Systematic Review and Meta-Analysis. *Journal of Critical Care*, **39**, 87-96. https://doi.org/10.1016/j.jcrc.2017.02.014

[11] Abrams, D., Baldwin, M.R., Champion, M., Agerstrand, C., Eisenberger, A., Bacchetta, M. and Brodie, D. (2016) Thrombocytopenia and Extracorporeal Membrane Oxygenation in Adults with Acute Respiratory Failure: A Cohort Study. *Intensive Care Medicine*, **42**, 844-852. https://doi.org/10.1007/s00134-016-4312-9

[12] Lindén, V., Palmér, K., Reinhard, J., Westman, R., Ehrén, H., Granholm, T. and Frenckner, B. (2000) High Survival in Adult Patients with Acute Respiratory Distress Syndrome Treated by Extracorporeal Membrane Oxygenation, Minimal Sedation, and Pressure Supported Ventilation. *Intensive Care Medicine*, **26**, 1630-1637. https://doi.org/10.1007/s001340000697

[13] Peek, G.J., Moore, H.M., Moore, N., Sosnowski, A.W. and Firmin, R.K. (1997) Extracorporeal Membrane Oxygenation for Adult Respiratory Failure. *Chest*, **112**, 759-764. https://doi.org/10.1378/chest.112.3.759

[14] Combes, A., Hajage, D., Capellier, G., Demoule, A., Lavoué, S., Guervilly, C., *et al.* (2018) Extracorporeal Membrane Oxygenation for Severe Acute Respiratory Distress Syndrome. *The New England Journal of Medicine*, **378**, 1965-1975. https://doi.org/10.1056/NEJMoa1800385

[15] Goligher, E.C., Tomlinson, G., Hajage, D., Wijeysundera, D.N., Fan, E., Jüni, P., *et al.* (2018) Extracorporeal Membrane Oxygenation for Severe Acute Respiratory Distress Syndrome and Posterior Probability of Mortality Benefit in a Post Hoc Bayesian Analysis of a Randomized Clinical Trial. *The Journal of the American Medical Association*, **320**, 2251-2259. https://doi.org/10.1001/jama.2018.14276

[16] Munshi, L., Walkey, A., Goligher, E., Pham, T., Uleryk, E.M. and Fan, E. (2019) Venovenous Extracorporeal Membrane Oxygenation for Acute Respiratory Distress Syndrome: A Systematic Review and Meta-Analysis. *The Lancet Respiratory Medicine*, **7**, 163-172. https://doi.org/10.1016/S2213-2600(18)30452-1

[17] Abrams, D. and Brodie, D. (2017) Extracorporeal Membrane Oxygenation Is First-Line Therapy for Acute Respiratory Distress Syndrome. *Critical Care Medicine*, **45**, 2070-2073. https://doi.org/10.1097/CCM.0000000000002734

[18] Lindén, V.B., Lidegran, M.K., Frisén, G., Dahlgren, P., Frenckner, B.P. and Larsen, F. (2009) ECMO in ARDS: A Long-Term Follow-Up Study Regarding Pulmonary Morphology and Function and Health-Related Quality of Life. *Acta Anaesthesiologica Scandinavica*, **53**, 489-495. https://doi.org/10.1111/j.1399-6576.2008.01808.x

International Journal of Clinical Medicine, 2021, 12, 279-296
https://www.scirp.org/journal/ijcm
ISSN Online: 2158-2882
ISSN Print: 2158-284X

Vascular Fractality and Alimentation of Cancer

Andras Szasz

Department of Biotechnics, St. Istvan University, Budaors, Hungary
Email: biotech@gek.szie.hu

How to cite this paper: Szasz, A. (2021) Vascular Fractality and Alimentation of Cancer. *International Journal of Clinical Medicine*, **12**, 279-296.
https://doi.org/10.4236/ijcm.2021.127025

Received: June 3, 2021
Accepted: July 13, 2021
Published: July 16, 2021

Abstract

Background: The basal metabolic rate has a scaling by tumor mass on the exponent of 3/4, while a simple surface-supplied volume of the mass would have a lower exponent, 2/3. The higher exponent can be explained by optimizing the overall energy distribution in the tumor, assuming that the target is four-dimensional. There are two possible ways of approximating the metabolic rate of the malignant tumor: 1) the volume blood-supply remains, but the surface and the length of the vessel network are modified; or 2) assuming that the malignant cell clusters try to maximize their metabolic rate to energize their proliferation by the longer length of the vessels. Our objective is to study how vascular fractality changes due to the greater demand for nutrients due to the proliferation of cancerous tissue. **Results**: It is shown that when a malignant tumor remains in expected four-dimensional volumetric conditions, it has a lower metabolic rate than the maximal metabolic potential in the actual demand of the proliferating cancer tissue. By maximizing the metabolic rate in malignant conditions, the allometric exponent will be smaller than 3/4, so the observed "dimensionality" of the metabolic rate versus mass becomes greater than four. The first growing period is exponential and keeps the "four-dimensional volume", but the growth process turns to the sigmoidal phase in higher metabolic demand, and the tumor uses other optimizing strategies, further lowering the scaling exponent of metabolic rate. **Conclusion**: It is shown that a malignant cellular cluster changes its metabolic scaling exponent when maximizing its energy intake in various alimentary conditions.

Keywords

Allometry, Metabolism, Fractal Dimensions, Optimization, Cancer, Vascularity

1. Introduction

The highly organized living systems are energetically open and far from thermal

equilibrium [1]. Its physical phenomena are collective and have strong physical roots [2]. Structures built up by anabolism and store information in the open system [3]. The living matter is heterogeneous, having numerous different electrolytes engulfed by specialized tissues or lipids enveloping isolated aqueous electrolytes in definite structures. The isolating layers control the chemical and physical reactions between the electrolytes and regulate the complex interactions. The fundamental division of electrolytes is between the cytosol (the intracellular electrolyte) and the Extracellular Matrix (*ECM*). The membrane is a complexly organized multifunctioning part. This double lipid layer regulates the information and ionic exchange between the intra and extracellular reagents, having a vital role in the energy distribution and production of the entire system. The mass of the living object is volume dependent (scaling by 3), while the surface is scaled only by 2. Consequently, we expect an exponent for mass-dependence of energy exchange (metabolism) as 2/3, the ratio of the cell surface to the cell volume ($\propto \frac{r^2}{r^3} = r^{2/3}$). So the expected metabolic power (P_{met}) in rest state (Basal Metabolic Power, *BMP*) dependence vs. mass (*M*) is expected:

$$P_{met} = BMP \propto M^{\frac{2}{3}} = M^{\alpha} \tag{1}$$

However, the experiments show a variation of exponents, the $\alpha = 2/3$ is not shared. When the metabolism is concentrated on surfaces, the $\alpha \approx 2/3$ well approaches reality. On the other hand, when it is centered on the energy resources, the exponent is close to $\alpha \approx 3/4$. When the whole mass of the organism is involved in the metabolic energy exchange, the exponent is near to $\alpha \approx 1$. In complete demand, the actual body-part (organ or whole-body) needs maximally available energy supply, proportional to its mass, so the scaling exponent is $\alpha = 1$ in this case [4]. In this case, the actual demand decides about the metabolic power and not the geometry. Of course, both the extremes are not ideal for the living object and could not follow evolutional requests. What is optimal? Despite the different exponential power, one feature is strictly common, all the experiments show power-scale (called scaling) in a few orders of magnitudes of the parameters, which is linear in the double logarithmic plot:

$$\ln\left(P_{met}\right) \propto \alpha \cdot \ln\left(M\right) \tag{2}$$

The scaling behavior is the consequence of the self-similarity of the living objects [5] [6]. The fundamental phenomenon behind it is the relative proportional change of the parameters [7]. The fundamental principle was oriented on the changes of the same organism, which has to grow in collective harmony, so the relative growth of parts must have balanced growth [8]. The structure and regulation of biosystems are complex. Various modern approaches have been developed in the last few decades to describe this complexity. The description of statistics of complex systems is far from the normal (Gaussian) distribution. Usually, power-law-tailed distributions (with a general exponent *α*) are applied:

$$f\left(x\right) = x^{\alpha} \tag{3}$$

There are various phenomena, including social, economic, physical, chemical, and biological, to be described by this function [9] [10] [11] [12] [13]. Despite the somewhat different fields of applications of the power law, it has a common root in complex systems: self-organization. The simplest fingerprint of the self-organized complexity is the self-similar or scale-free structures characterized by a power function. This power-function relation magnifies the $f(x)$ by a constant only, m-dependent $\Xi = m^{\alpha}$ value at any m magnification of x:

$$f(mx) = (mx)^{\alpha} = m^{\alpha}x^{\alpha} = \Xi x^{\alpha} = \Xi f(x) \tag{4}$$

Self-organization explains the evolution of the system [14], expressed in non-linear dynamics [15].

The objective of this present article focuses on analyzing the metabolic alimentation of the healthy tissues in normal conditions and the developing tumors in two different conditions:

1) When the tumor metabolizes as a homeostatic organized unit, the theoretically expected allometric exponent corresponds with the optimal healthy allometry;

2) When the tumor metabolism is not in such an "ideal" optimization of the metabolic supply, its alimentation is suboptimal, using the observed fractal behavior of its angio-structure.

2. Method

Fractal physiology describes the structural and dynamical properties of living organisms and their parts [16] [17], based on physical principles [18]. The self-similar behavior could be described by the normalized relative change of the magnitudes, similarly to the Weber-Fechner law [19] in psychophysics like:

$$\frac{\Delta f}{f} = \alpha \frac{\Delta x}{x} \tag{5}$$

where α is a constant fitting factor. By integration, we get the (3):

$$\ln(f) = \alpha \ln(x) \rightarrow f(x) = x^{\alpha} \tag{6}$$

The self-similar functional relation makes a "scale-invariance" feature due to the independence of the magnification, which is the fundamental behavior of the fractal structures, too [20].

The power function is the central description of the scaling in (1), which bases the allometry of living organisms [21]. The original allometry idea was recognized almost a hundred years ago [22], but the exciting question of the energizing of the life phenomena explained in connection of allometry is a half-century-old knowledge [23]. The connection between the homeostatic energizing level and the basal metabolic rate (B_0) as a self-similar function of mass (m) of living objects is [24]:

$$B_0 = am^{\alpha} \tag{7}$$

where the two parameters are determined experimentally; a is the allometric coefficient, and α is the allometric exponent, and (7) is usually called bioscaling [25]. The usual regression analysis uses the logarithmic transformation of (7):

$$\ln B_0 = \alpha \ln(m) + \ln(a) \tag{8}$$

which allows high linear accuracy and fits both parameters a and α well [26]. The literature has numerous debates about the theoretical allometric relation based on fractal calculus and the empirical fits based on probability calculus [27]. The B_0 of living objects shows allometric scaling to its mass, which refers to the energy supply of the living mass of the volume. The (7) function gives a correct mathematical and biological framework for the complex bio-systems fractal studies [28]. The scaling power function of the mass describes it, and it has been shown valid in a broad category of living structures and processes [29]. The scaling considerations are applied not only in biology but broader, in the complete biosystem as well [30]. The importance of understanding the challenges of the complexity of human medicine was recognized on this basis [31] [32].

In a simple formulation, metabolic processes are surface-dependent, while the mass is proportional to the volume. Therefore, the exponent of their ratio mirrors their dimensionality, and consequently, the exponent is 2/3 [33]. Complex living allometry most likely shows the exponent as 3/4 instead of 2/3 in a broad spectrum of living objects [34], or at least have no linearity in a double-logarithmic plot [35]. However, the large data-mining does not show an overall validity of the 3/4 exponent over 2/3 [36]. The curvature could be size-dependent in developing clusters by their size [37]. The 3/4 exponent could be described as a relation between the three-dimensional surface and the four-dimensional volume [38]. The explanation of the fourth dimension is based on the fractal structure of microcirculation [39], which supplies the energy demand according to a homeostatic equilibrium (B_0) in the living complexity. Life in this meaning is "four-dimensional". Its metabolic exchange processes proceed on fractal surfaces, maximizing the available energy consumption, scaling even the fluctuation of the metabolic power in the universal scaling law as well [40].

The optimization of energy consumption was formulated rigorously by the scaling idea and discussed in a universal frame, even on the energy-consumption subcellular level, including the mitochondria and respiratory complexes [41]. The allometry shows a structural, geometrical constraint for living organisms in homeostatic equilibrium.

The metabolic scaling in cancer development is critical [42]. Contrary to the homeostatic homogeneity of the healthy tissue [43]; the functional heterogeneity of the solid tumor allows an abnormal organ self-possession of multiple cell-types and electrolytes like the Extracellular Matrix (*ECM*) lymph and blood-transports [44]. The tumor metabolism is based on the blood transport to the tumor. The logarithm of wet-weight of the tumor (m_{wet}) and the tumor blood-flow (B_t) have linear dependence [45], which was observed in model xenografts of ovarian cancer, so they have a bioscaling relation:

$$\log\left(B_t\right) = -0.808\log\left(m_{wet}\right) - 0.436,\ r^2 = 0.79,\ p < 0.001$$
$$\left[B_t = 0.6466 \cdot m_{wet}^{-0.808}\right] \tag{9}$$

where the exponent is close to 3/4.

The allometric scaling supposes three geometrical variables to define the optimization of the circulatory system in living objects:

- The average length of the blood circulatory network (l);
- The surface of the relevant material exchange of the blood circulation system (s);
- The volume of the blood (v).

Furthermore, we suppose that these parameters are represented by the self-similar, self-organized functions of the L value, which is characteristic of a given organ. Hence:

$$l \propto L^{a_l},\ s \propto L^{a_s},\ v \propto L^{a_v} \tag{10}$$

Using the theoretical fractal explanation, the conditions are: $a_l \geq 1$, $a_s \geq 2$ and $a_v \geq 3$, from where:

$$l \propto L_0^{1+\varepsilon_l},\ s \propto L_0^{2+\varepsilon_s},\ v \propto L_0^{3+\varepsilon_v} \tag{11}$$

where $0 \leq \varepsilon_l \leq 1$, $0 \leq \varepsilon_s \leq 1$, and L_0 is the characteristic length. The first relation limits the pattern of the circulatory system to the maximum that could be planar, while the second is limited to a maximum, filling up a three-dimensional space. The third exponent ε_v could be calculated because the exponents are not independent. The volume is proportional to the product of the surface and length:

$$v \propto s \times l \tag{12}$$

consequently

$$\varepsilon_v = \varepsilon_l + \varepsilon_s \tag{13}$$

Using these conditions, we obtain from (11):

$$L_0 \propto v^{\frac{1}{3+\varepsilon_v}} \rightarrow s \propto v^{\frac{2+\varepsilon_s}{3+\varepsilon_v}} \tag{14}$$

Furthermore, the actual volume of the blood is proportional to the actual mass of the given system or organ:

$$v \propto L_0^{3+\varepsilon_v} \propto m^1 \tag{15}$$

Considering (14) and (15), now we have:

$$s \propto m^{\frac{2+\varepsilon_s}{3+\varepsilon_l+\varepsilon_s}} \tag{16}$$

The metabolism is a surface-controlled mechanism, so $\left(BMR\right) \propto s$, consequently:

$$B_0 \propto m^{\frac{2+\varepsilon_s}{3+\varepsilon_l+\varepsilon_s}} \tag{17}$$

If the living structure is geometric in conventional Euclidean meaning, then

$\varepsilon_l = \varepsilon_s = \varepsilon_v = 0$ and therefore $a_l = a_s = a_v$; consequently, the scaling is $(BMR) \propto m^{\alpha}$, where $\alpha = \frac{2+\varepsilon_s}{3+\varepsilon_l+\varepsilon_s} = 2/3$. When at least one of the $\varepsilon_l \neq 0$, $\alpha \neq 2/3$, which modifies the common simple dimensional approach of the metabolic processes.

3. Results

The allometry gives a possibility to describe the development of the tumor [46]. It is valid for the primary cancer lesions but not always applicable in metastases [47]. We are dealing with primary tumors only. There are two ways of approximating the allometric metabolic rate of a tumor:

1) The theoretical approach accepts that a healthy life has a four-dimensional behavior connected to the highly self-organized, consequently self-similar hierarchic order [48], we fix the exponent to 3/4.

2) The experimental approach assumes that the cell cluster tries to maximize its metabolic rate [49], and this way, it modifies the scaling exponent from the value of 3/4.

Both approaches depend on the environmental conditions of the tumor, mainly on the nourishment of the cells.

3.1. Optimal Alimentation to Maximum Metabolic Rate

Evolution maximized the surface where the nutrients are transferred from the blood to the cells, ensuring the best conditions of the living object, so:

$$s(\varepsilon_l, \varepsilon_s) = \max \tag{18}$$

This task is equivalent to the minimizing of the reciprocal value of the exponent in (16):

$$\frac{3+\varepsilon_l+\varepsilon_s}{2+\varepsilon_s} = \min \tag{19}$$

with constraint conditions of:

$$0 \le \varepsilon_l \le 1, \ 0 \le \varepsilon_s \le 1 \tag{20}$$

(19) can be transformed into

$$\frac{3+\varepsilon_l+\varepsilon_s}{2+\varepsilon_s} = 1 + \frac{1+\varepsilon_l}{2+\varepsilon_s} = \min \tag{21}$$

Hence, considering (20), the minimum condition demands that:

$$\varepsilon_l = 0, \ \varepsilon_s = 1 \tag{22}$$

Substituting (22) into (11), the exponents of the self-similar structures are:

$$l \propto L_0^1, \ s \propto L_0^3, \ v \propto L_0^4 \tag{23}$$

Consequently, in cases of ideal alimentation, these exponents are the fractal dimensions of the parameters of the network, and while the length is one dimensional, the surface is three, and the volume is four [38]. Because metabolism

is a surface-regulated process, $s \propto (BMR)$, the scaling exponent of the metabolic rate versus mass using (16) is 3/4:

$$B_0 \propto s \propto m^{\frac{2+\varepsilon_s}{3+\varepsilon_l+\varepsilon_s}} = m^{\frac{3}{4}} \tag{24}$$

and so B_0 in the unit mass

$$\frac{B_0}{m} \propto m^{-\frac{1}{4}} \tag{25}$$

Primarily the blood stream provides the metabolic supply, so the fractality of the vascular network could be decisional in its allometric evaluation. The condition of (24) maximizes the blood flow energizing all the parts of the volume for their optimum, providing a maximum metabolic rate.

In consequence of (24), the life prefers the large masses as more effective energy-consumers in a unit volume shown in (25). However, on another side this process could lead to the loss of complex information, developing higher instability of the system, arguing that this is a negative tendency manifest the "aging of life's algorithm as a whole" [50]. The model could be applied by guessing when the energy supply is optimal, so the developed active surface cannot supply the actual demands. Two different sources are possible to create such a situation (1) the length of the supplier system changes (the constructional template differs), or (2) the volume of transport exchange is limited despite the growing demands. Various irregularities originate both challenges could be a symptom of disease, like cancer [51].

3.2. Suboptimal Alimentation for Tumor

The malignancy usually demands a higher energy input from its healthy environment than the available. The tumor supply is suboptimal. The higher energy demand (usually exponential in starting phase [52]) forces to increase the length of the vessel network. In cancerous clusters, contrary to (22), the vascular fractal dimension (D_v) of the supplying blood-vessel network ($l \propto L_0^{D_v}$) is larger than 1, ($D_v \geq 1$) [51]; consequently $\varepsilon_l \neq 0$ in the relation of (11). D_v could be measured by the box-counting method [51].

According to (11), the actual active surface is evolutionary normal for self-organizing of healthy tissues ($s \propto L_0^3$). The extra energy demand of the intensive proliferation changes the exponents of parameters in (11). In this case, the surface of the supply follows the evolution-requested exponent of 3 ($\varepsilon_s = 1$ from (22)) in the self-similar conditions, but the requested length changes:

$$l \propto L_0^{1+\varepsilon_l} = L_0^{D_v}, \; s \propto L_0^3 \tag{26}$$

where $\varepsilon_l > 0$ modifies the power of the transport measures, so the fractal organization of the transport lines is different. This type of change could be formed by neoangiogenesis satisfying the higher energy demand in cancerous tissues and could cause abnormalities as inflammation, thrombosis, varicose veins modification of the arteries, etc. The corresponding power-law for the ac-

tual metabolic rate at the longer length of vessels, so the suboptimal metabolic rate in this phase (B_{so1}) from (24) is:

$$B_{so1} \propto m^{\frac{2+\varepsilon_s}{3+\varepsilon_l+\varepsilon_s}} = m^{\frac{3}{4+\varepsilon_l}} = m^{\frac{3}{3+D_v}} \tag{27}$$

The apparent "dimension" of the reaction request for volume is $(4+\varepsilon_l)>4$, the dimension increases. According to $l \propto L_0^{1+\varepsilon_l}$ the measurable fractal dimension of the blood vessel network is $D_v = 1+\varepsilon_l$. In this way the ε_l is measurable by the fractal dimension of the vessel structures [53], for example, with the box-counting method [51]. When $D_v = 1.3$ [53], $\varepsilon_l = 0.3$, and the scaling exponent is $\alpha \cong 0.7 > 2/3$. The Microvessel Fractal Dimension (*MFD*) (which is equivalent with $(1+\varepsilon_l)$ for renal cell carcinoma ranges between 1.30 - 1.66 [54], and correlates well with the tumor Microvessel Density (*MVD*) [54]. From (27) we know, when $\varepsilon_l = 0.478$, the scaling exponent describes a non-fractal-like structure, $\alpha = 2/3$.

When the tumor growth is so intensive that the available length of the vessel network cannot deliver appropriate energy, then another possible deviation from the homeostatic self-organization happens. In this case, the volume of the delivered energy remains constant, which limits the energy supply. The tumor-growth turns to sigmoidal this stage [55], usually follows Weibull distribution due to the self-similar development [6]. This could happen in severe hypoxia, low oxygen saturation in blood, anemia, various hematological diseases. In this case, the volume of the supply follows the evolution-requested exponent of 4 ($\varepsilon_v = 1$) (23), in the self-similar conditions in [53], but the requested length and surface is not enough for the proper work, so $\varepsilon_l' > 1$ and $\varepsilon_s < 1$. The self-similar conditions differ from (22) due to (13):

$$l \propto L_0^{1+\varepsilon_l'},\ s \propto L_0^{3-\varepsilon_l'},\ v \propto L_0^4 \tag{28}$$

Consequently, at fixed four-dimensional volume, the metabolic surface reactions behave by power-law of suboptimal metabolic rate in this phase:

$$B_{so2} \propto m^{\frac{2+\varepsilon_s}{3+\varepsilon_l'+\varepsilon_s}} = m^{\frac{3-\varepsilon_l'}{4}} = m^{\frac{4-D_v'}{4}} \tag{29}$$

Here the volume "dimension" of the reaction request is 4, but the actual conditions are worse than optimal. The ε_l' again here also is measurable by the fractal dimension of the structures [56], in this case, the fractal dimension of the vessel system is $D_v' = 1+\varepsilon_l'$. For example, measuring the vascular fractal dimension in one disease as $D_v' = 1.41$ [51], we use $\varepsilon_l' = 0.41$, so the scaling exponent is $\alpha = 0.65$. When $\varepsilon_l' = 0.28$ [56], the scaling exponent is $p = 0.68$. At $\varepsilon_l' = 0.33$, the scaling exponent is the well-known $\alpha = 2/3$.

The exponents of the active transport surface in the two suboptimal supplies

$$\alpha = \frac{3}{4+\varepsilon_l} = \frac{3}{3+D_v} \text{ and } \alpha' = \frac{3-\varepsilon_l'}{4} = \frac{4-D_v'}{4} \tag{30}$$

Both these exponents are smaller than the optimal, and the exponent in the second phase of growth is the smallest (**Figure 1**).

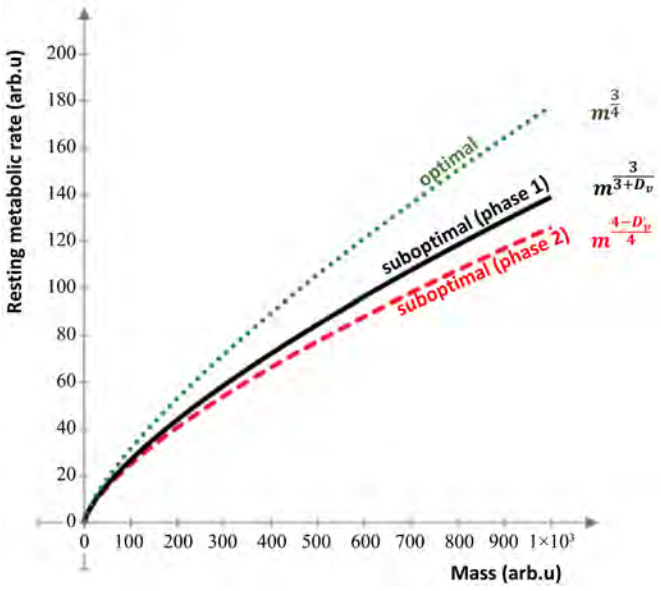

Figure 1. The allometric development with the various exponents. The initial phase of tumor growth is exponential, and the allometric scale follows the phase1 curve, while the intensive development further decreases the exponent, which turns to a sigmoid phase in a tumor-specific time.

Following the idea of "4-dimensionality", the volume dimension changes in α, while the active surface in α'. Both exponents are ≤3/4 because of the length fractal dimension >1. The mechanisms which cause this modification are different. The same exponent could be only in Euclidean non-fractal case, when $D_v = D_v' = 1$. Due to $D_v < 3$ and $D_v' < 3$, hence $\alpha > 0.5$ and $\alpha' > 0.25$. The Mandelbrot calculated 2.7 for the fractal dimension of the arterial tree of the lung [57], which was supported by experiments later [58], the relevant changes are $\alpha \approx 0.526$ and $\alpha' \approx 0.325$. Both values are smaller than $\alpha = 2/3$.

Both non-optimal situations (defect of the length of transport way or limited transport against the demands) make the tissue under-energized, and the exponent of the power-relation scaling down-regulated. In such a way, measuring the scaling exponent of metabolism and the fractal dimension of the supplying microvessels have a diagnostic value about the actual deviations from normal.

4. Discussion

The optimal alimentation in a healthy system makes the energy distribution balanced, supplying all requirements of the homeostatic state. The exponent 3/4 has a strong predominance on a theoretical and empirical basis [59] in healthy homeostatic basal metabolic activity. The ideal nutrition supply supports ontogenic growth. However, at least at larger sizes, the cancer growth never happens with an optimal nutrition supply; the cells compete intensively for the available energy sources.

The cancer is out of the overall homeostatic balance. The tumor development certainly has a higher energy supply due to its proliferation than its healthy

counterpart needs. Due to the extra-large energy demand, the tumor development's alimentation in most cases is far from optimal, so the tumor is in a permanent energy deficiency. When the oxygen supply is limited, the first attempt to produce more ATP is the massive fermentative use of glucose, a simple and quick production mechanism. The cell extends its ATP production to fermentation by non- mitochondrial respiration, abandoning the more complicated Kerbs-cycle in the mitochondria [60].

While the mitochondrial metabolism is always aerobic, its scaling exponent is nearly $\alpha = 3/4$ [30]. However, the scaling of metabolic activity is also different in mitochondrial and non-mitochondrial processes [61]. The metabolic power not only depends on the active surface of the transport but also on the transport rate at the same active surface size. Due to the transport modifications at the changed metabolic pathway, the deviation from the 3/4 exponent could be remarkable. The allometric scaling exponent of fermentative processes decreases to nearly 2/3. This last scaling exponent shows that the cell-membrane directly regulates the fermentation, and the surface/volume ratio controls the complete process, which could be anticipated from the direct linear dependence of the lactate production (V_L) on the glucose-intake (V_G) with a slope of ≅1 [45]:

$$\log\left(V_L\right) = +0.977\log\left(V_G\right) + 0.108,\ r^2 = 0.72,\ p < 0.001 \tag{31}$$

while the bioscaling of the oxygen (V_{O_2}) and glucose (V_G) intake [45] are even lower than 2/3, −0.570, and −0.523, respectively.

Not only does the malignancy need an intensive extra metabolism. For example, the benthic invertebrates ($n = 215$) have the lowest average scaling exponent ($\alpha_{\text{mean}} = 0.63$, [near to 2/3], $CI_{\text{mean}} = 0.18$), which metabolizes in an anaerobic way [62]. No regulative factor exists when the cells are entirely independent, and the available alimentation is unlimited (like in most in vitro experiments). The metabolic rate is linearly proportional to the mass, so the exponent is $\alpha \cong 1$ [30].

The metabolic transformation of the cells [63] is one of the well-recognized hallmarks of malignancy [64] that has an emerging intensive interest in the field of oncology [65], as the core hallmark of cancer [66]. The adaptation of mitochondria in energy-limited conditions is the focus of the research [67]. The tumor forces the development of the angiogenetic processes [68] and overcomes the energy limitations. The vascularity is promoted [69], and the rapid development by intensive proliferation supports the changes of the scaling behavior [70]. Without extra angiogenesis (starting clusters), only the ready-made capacity of the delivery is available, so the tumor has a suboptimal alimentation. In the beginning, its fractal structure was developed, which is similar to the healthy structure, so the four-dimensional scaling remains valid (28).

When the tumor develops, the fractal structure of vascularity changes. Consequently, its fractal dimension changes too. The forced angiogenesis [68] tries to provide a sufficient supply to the hypoxic (insufficiently supported) tumor, and the structure changes rapidly, broadening the scaling exponent in a wide range [71]. The missing supply suppresses the scaling exponent, shown in (27).

Still, the angiogenetic pool changes the trend, approaching linearity. The unlimited availability of nutrients for every cell realizes the linearity measured in vitro [48], limited to ~0.9 in vivo by insufficient oxygen transport [72]. However, the angiogenesis is usually not fast enough to supply the faster-growing larger tumors, so the inner part of the tumor becomes necrotic, forming a smaller living mass to supply, easing the energy distribution [68]. The essential message of the cases of insufficient alimentation from the calculations above is that when the fractal dimension of the supplying network grows, the scaling exponent decreases. The four-dimensionality and the allometry with the evolutional optimizing request are not the same approaches: further evolution conditions have a higher than four-dimensional allometric scaling. The tumor mass is a somewhat indefinite parameter because the whole environment of the tumor suffers from suboptimal alimentation. Consequently, we tried to find a more fundamental networking condition parameter published elsewhere [73].

There is a vast number of researches about the vascular development of the tumor progression, calculating the fractal dimension of the vascularity. The in silico modeling of the growing tumor vessel architecture in high-grade gliomas [74] shows that the fractal dimension is less than 1 in the avascular state and growing linearly by time, reaching $D_{t=2760\,\mathrm{h}} \cong 1.2$ at $t = 2760\,\mathrm{h}$, by slope approximately $\cong 6.2\times10^{-4}$. In a longer time, the development of the fractal dimension drastically changes, follows a less rapid development (slope $\cong 2.5\times10^{-4}$) until $D_{t=4000\,\mathrm{h}} \cong 1.48$. We may assume that the fractal dimension 1.2 characterizes the finally developed vessel structure inside the tumor, followed by neo-angiogenetic processes reaching the tumor-surface, changing the vascular architecture, growing slower to the higher values of the fractal dimension.

In optimal alimentation, the allometric scaling shows exponent 3/4 (24); which supposes the $l \propto L_0^1$, so the vascular fractal dimension in this case is $D_{va} = 1$. However $D_{va} > 1$ by the growing vessel network, so $\alpha < 3/4$ in the allometric scaling of tumor-vascularity due to the suboptimal energy supply, which triggers the angiogenesis. Using the results from in silico model-calculations, the internal growth of the vessels have $(B_0)_{i1} \propto m^{\frac{2.8}{4}} = m^{0.700}$, or $(B_0)_{i2} \propto m^{\frac{3}{4.2}} = m^{0.714}$, according to the assumption of suboptimal alimentation by maximal metabolic rate (case 1) or by the metabolic rate forced four-dimensional "optimizing" concept (case 2). When the external angiogenesis is developing, the allometry changes: $(B_0)_{e1} \propto m^{\frac{2.52}{4}} = m^{0.63}$, and $(B_0)_{e2} \propto m^{\frac{3}{4.48}} = m^{0.67}$. So, the optimizing of the suboptimal energy availability in extended angiogenetic cases realizes the allometry, which fits the simple geometrical expectations $\alpha = 2/3$ well.

The measurements of vascular fractal dimensions in various tumors show a lower scaling exponent than the ideal 3/4, depending on the conditions of the tumor-angiogenesis development. For example, when the epithelial-connective tissue interfaces with a malignant tumor in the oral mucosa, it is $D_{va} \geq 1.41$ [75], the scaling exponent in suboptimal alimentation situations in cases 1 and 2

are $\alpha \cong 0.64$ and $\alpha = 0.68$. The last one (optimal distribution of the suboptimally available energy) is near the "conventional" 2/3. Another microscopic evaluation of angio-structures [76] shows lower values of α, like the fractal dimension of the normal and malignant tissues are $D_{\text{healthy}} \cong 1.65$ and $D_{\text{malignant}} \cong 1.74$, respectively [77]; resulting in low α values. In other evaluations, the vascular structure's dimensionality grows to 1.9, which provides the maximal energy usage of the suboptimal alimentation, and the exponent became as low as $\alpha = 0.525$.

It is interesting to see the effect of various anti-tumor treatments on the vascular fractal dimension. The treatment changes the vascularization and suppresses the fractal dimension forms 1.135 1.037, 0.933, 0.982 by Photodynamic Therapy (PDT); Cysteine Proteases Inhibitors (CPI), combined therapy, PDT and CPI [78]; which corresponds in cases when the maximalizing of the energy-supply is equivalent to the allometric exponents of 0.716, 0.741, 0.767 and 0.755, respectively (the optimal distribution of the suboptimal availability would be 0.726, 0.743, 0.763, and 0.753). By treating VEGF165, the fractal dimension increases from 1.65 to 1.69, decreasing the allometric exponent [79] [80]. In matrigel inoculated human umbilical vein endothelial cells (HUVEC) treated by docetaxel, the fractal dimension of the vascular structure has decreased from 1.2 to 1.09, corresponding in case 1 $\alpha_{\text{control}} \cong 0.70; \alpha_{\text{treated}} \cong 0.73$, and in case 2 $\alpha_{\text{control}} \cong 0.71; \alpha_{\text{treated}} \cong 0.73$ [81]. The fractal analysis is a successful and rather accurate method for monitoring the efficacy of angiogenic consequences of therapies [82].

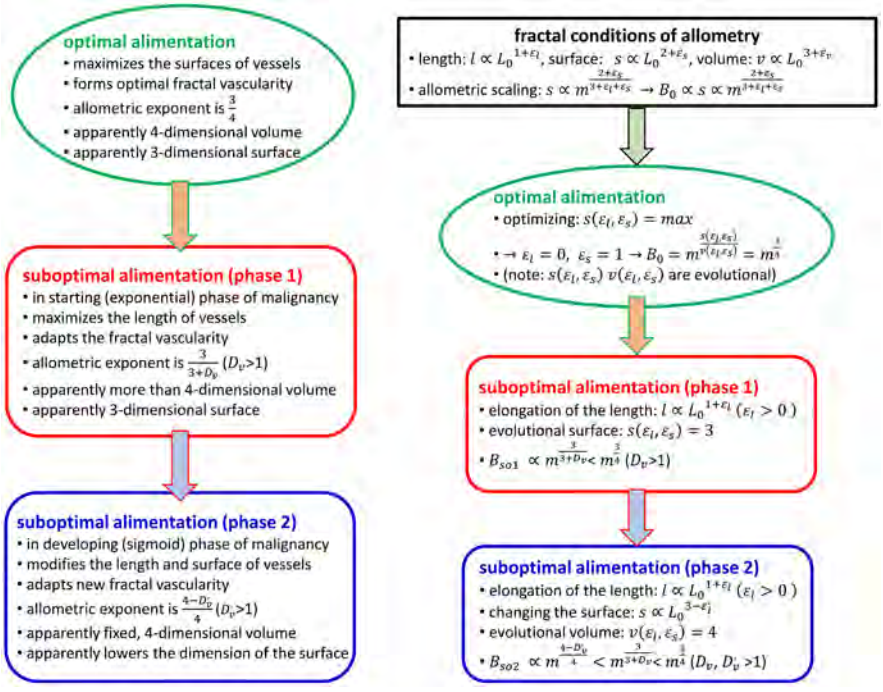

Figure 2. The summary of the structure of calculation. (a) The biophysical considerations (b) The mathematical description.

5. Summary

We had shown that the allometric relation of basal metabolic rate and the tumor mass depends on the fractal dimension of the vascular structure. Due to the desperate need for energy supply and the intensive proliferation of the malignant tumor, cancer does not have an optimal alimentation. Two strategies could distribute the available (not sufficient) energy by the main transport of it, the vascular network:

1) Assuming that the cell cluster tries to maximize its metabolic rate by the surface transports and lowers the scaling exponent from the value of 3/4;

2) Accepting that in the case of a four-dimensional volumetric behavior limits the energy supply. The tumor optimizes the energy distribution in its volume in among these conditions.

The structure of the biophysical considerations and their mathematical steps are summarized in **Figure 2**.

The two strategies in consequent phases of tumor growth optimize the available energy by different allometric scalings. The organized optimum of the suboptimal availability of energy gives lowered allometric scaling exponents.

Acknowledgements

This work was supported by the Hungarian National Research Development and Innovation Office PIACI KFI grant: 2019-1.1.1-PIACI-KFI-2019-00011.

Conflicts of Interest

The author declares no conflicts of interest regarding the publication of this paper.

References

[1] Barge, L.M., Branscomb, E., Brucato, J.R., Cardoso, S.S.S., Cartwright, J.H.E., Danielache, S.O., *et al.* (2017) Thermodynamics, Disequilibrium, Evolution: Far-From-Equilibrium Geological and Chemical Considerations for Origin-Of-Life Research. Origins of Life and Evolution of the Biospheres. *The journal of the International Society for the Study of the Origin of Life*, **47**, 39-56. https://doi.org/10.1007/s11084-016-9508-z

[2] Goldenfeld, N. and Woese, C. (2011) Life Is Physics: Evolution as a Collective Phenomenon Far from Equilibrium. *Annual Review of Condensed Matter Physics*, **2**, 375-399. https://doi.org/10.1146/annurev-conmatphys-062910-140509

[3] Schrodinger, E. (1944) What Is Life? The Physical Aspect of the Living Cell. Cambridge University Press, Cambridge.

[4] Glazier, D.S. (2008) Effects of Metabolic Level on the Body Size Scaling of Metabolic Rate in Birds and Mammals. *Proceedings of the Royal Society B*: *Biological Sciences*, **275**, 1405-1410. https://doi.org/10.1098/rspb.2008.0118

[5] Szasz, O., Szigeti, G.P. and Szasz, A. (2017) On the Self-Similarity in Biologyical Processes. *Open Journal of Biophysics*, **7**, 183-196. https://doi.org/10.4236/ojbiphy.2017.74014

[6] Szasz, O. and Szasz, A. (2020) Parametrization of Survival Measures, Part I: Conse-

quences of Self-Organizing. *International Journal of Clinical Medicine*, **11**, 316-347. https://doi.org/10.4236/ijcm.2020.115031

[7] Huxley, J.S. and Teissier, G. (1936) Terminology of Relative Growth. *Nature*, **137**, 780-781. https://doi.org/10.1038/137780b0

[8] Huxley, J.S. (1932) Problems of Relative Growth. Book Review by C.H.K. in Gahan: New Parasitic Ilymenoplera, Lincoln Mac Veagh—The Dial Press, New York, 757.

[9] Newman, M.E.J. (2005) Power Laws, Pareto Distributions and Zipf's Law. *Contemporary Physics*, **46**, 323-351. https://doi.org/10.1080/00107510500052444

[10] Mitzenmacher, M. (2004) A Brief History of Generative Models for Power Law and Lognormal Distributions. *Internet Mathematics*, **1**, 226-251. https://doi.org/10.1080/15427951.2004.10129088

[11] Fisher, M.E. (1998) Renormalization Group Theory: Its Basis and Formulation in Statistical Physics. *Reviews of Modern Physics*, **70**, 653-681. https://doi.org/10.1103/RevModPhys.70.653

[12] Barabasi, A. and Albert, R. (1999) Emergence of Scaling in Random Networks. *Science*, **286**, 509-512. https://doi.org/10.1126/science.286.5439.509

[13] Chignola, R., Sega, M., Stella, S., Vyshemirsky, V. and Milotti, E. (2014) From Single-Cell Dynamics to Scaling Laws in Oncology. *Biophysical Reviews and Letters*, **9**, 273-284. https://doi.org/10.1142/S1793048014300035

[14] Kauffman, S.A. (1992) The Origins of Order: Self-Organization and Selection. In: Varela, F.J. and Dupuy, J.P., Eds., *Understanding Origin*, Vol. 130, Springer, Dordrecht, 153-181. https://doi.org/10.1007/978-94-015-8054-0_8

[15] Walleczek, J. (Ed.) (2000) Self-Organized Biological Dynamics & Nonlinear Control. Cambridge Univesity Press, Cambridge. https://doi.org/10.1017/CBO9780511535338

[16] Bassingthwaighte, J.B., Leibovitch, L.S. and West, B.J. (1994) Fractal Physiology. Springer, New York. https://doi.org/10.1007/978-1-4614-7572-9

[17] Deering, W. and West, B.J. (1992) Fractal physiology. *IEEE Engineering in Medicine and Biology*, **11**, 40-46. https://doi.org/10.1109/51.139035

[18] Musha, T. and Sawada, Y., Eds. (1994) Physics of the Living State. IOS Press, Amsterdam.

[19] Fechner, G.T., Howes, D.H. and Boring, E.G., Eds. (1966) Elements of Psychophysics. Volume 1, Adler, H.E., Trans., Holt, Rinehart and Winston, New York.

[20] Mandelbrot, B.B. (1967) How Long Is the Coast of Britain? Statistical Self-Similarity and Fractional Dimension. *Science*, **156**, 636-638. https://doi.org/10.1126/science.156.3775.636

[21] West, B.J. and West, D. (2012) Fractional Dynamics of Allometry. *Fractional Calculus & Applied Analysis*, **15**, 70-96. https://doi.org/10.2478/s13540-012-0006-3

[22] Huxley, J.S. (1932) Problems of Relative Growth. Johns Hopkins University Press, Methuen, London, 273.

[23] Kleiber, M. (1961) The Fire of Life: An Introduction to Animal Energetics. Wiley, New York.

[24] Savage, Van M., Allen, A.P., Brown, J.H., Gillooly, J.F., Herman, A.B., Woodruff, W.H. and West, G.B. (2007) Scaling of Number, Size, and Metabolic Rate of Cells with Body Size in Mammals. *Proceedings of the National Academy of Sciences of the United States of America*, **104**, 4718-4723. https://doi.org/10.1073/pnas.0611235104

[25] Brown, J.H. and West, G.B., Eds. (2000) Scaling in Biology. Oxford University Press, Oxford.

[26] Mascaro, J., Litton, C.M., Hughes, R.F., Uowolo, A. and Schnitzer, S.A. (2014) Is Logarithmic Transformation Necessary in Allometry? Ten, One-Hundred, One-Thousand-Times Yes. *Biological Journal of the Linnean Society*, **111**, 230-233. https://doi.org/10.1111/bij.12177

[27] West, D. and West, B.J. (2012) On Allometry Relations. *International Journal of Modern Physics B*, **26**, Article ID: 1230010. https://doi.org/10.1142/S0217979212300101

[28] Brown, J.H., West, G.B. and Enquis, B.J. (2005) Yes, West, Brown and Enquist's Model of Allometric Scaling Is Both Mathematically Correct and Biologically Relevant. *Functional Ecology*, **19**, 735-738. https://doi.org/10.1142/S0217979212300101

[29] Calder III, W.A. (1984) Size, Function and Life History. Dover Publications Inc., Mineola, New York.

[30] West, G.B. and Brown, J.H. (2005) The Origin of Allometric Scaling Laws in Biology from Genomes to Ecosystems: Towards a Quantitative Unifying Theory of Biological Structure and Organization. *Journal of Experimental Biology*, **208**, 1575-1592. https://doi.org/10.1242/jeb.01589

[31] West, B.J. (2006) Where Medicine Went Wrong: Rediscovering the Path to Complexity. Vol. 11, World Scientific Publishing Co. Pte. Ltd., New Jersey, London. https://doi.org/10.1142/6175

[32] West, B.J. (1990) Fractal Physiology and Chaos in Medicine. World Scientific, Singapore, London.

[33] White, C.R. and Seymour, R.S. (2003) Mammalian Basal Metabolic Rate Is Proportional to Body Mass2/3. *Proceedings of the National Academy of Sciences of the United States of America*, **100**, 4046-4049. https://doi.org/10.1073/pnas.0436428100

[34] Moses, M.E., Hou, C., Woodruff, W.H., West, G.B., Nekola, J.C., Wenyun Zuo, *et al.* (2008) Revisiting a Model of Ontogenic Growth: Estimating Model Parameters from Theory and Data. *American Naturalist*, **171**, 632-645. https://doi.org/10.1086/587073

[35] Kolokotrones, T., Savage, Van M., Deeds, E.J. and Fontana, W. (2010) Curvature in Metabolic Scaling. *Nature*, **464**, 753-755. https://doi.org/10.1086/587073

[36] Dodds, P.S., Rothman, D.H. and Weitz, J.S. (2001) Re-Examination of the "3/4-Law" of Metabolism. *Journal of Theoretical Biology*, **209**, 9-27. https://doi.org/10.1006/jtbi.2000.2238

[37] Milotti, E., Vyshemirsky, V., Stella, S., Dogo, F. and Chignola, R. (2017) Analysis of the Fluctuations of the Tumour/Host Interface. *Physica A. Statistical Mechanics and its Applications*, **486**, 587-594. https://doi.org/10.1016/j.physa.2017.06.005

[38] West, G.B., Brown, J.H. and Enquist, B.J. (1999) The Four Dimension of Life: Fractal Geometry and Allometric Scaling of Organisms. *Science*, **284**, 1677-1679. https://doi.org/10.1126/science.284.5420.1677

[39] West, G.B., Brown, J.H. and Enquist, B.J. (1997) A General Model for the Origin of Allometric Scaling Laws in Biology. *Science*, **276**, 122-126. https://doi.org/10.1126/science.276.5309.122

[40] Labra, F.A., Marquet, P.A. and Bozinovic, F. (2007) Scaling Metabolic Rate Fluctuations. *Proceedings of the National Academy of Sciences of the United States of America*, **104**, 10900-10903. https://doi.org/10.1073/pnas.0704108104

[41] West, G.B., Woodruff, W.H. and Brown, J.H. (2002) Allometric Scaling of Metabolic Rate from Molecules and Mitochondria to Cells and Mammals. *Proceedings of the National Academy of Sciences of the United States of America*, **99**, 2473-2478. https://doi.org/10.1073/pnas.012579799

[42] Guiot, C., Delsanto, P.P.P., Carpinteri, A., Pugno, N., Mansury, Y. and Deisboeck, T.S. (2006) The Dynamic Evolution of the Power Exponent in a Universal Growth Model of Tumors. *Journal of Theoretical Biology*, **240**, 459-463. https://doi.org/10.1016/j.jtbi.2005.10.006

[43] Puliafito, A., Primo, L. and Celani, A. (2017) Cell-Size Distribution in Epithelial Tissue Formation and Homeostasis. *Journal of The Royal Society Interface*, **14**, Article ID: 20170032. https://doi.org/10.1098/rsif.2017.0032

[44] Egeblad, M., Nakasone, E.S. and Werb, Z. (2010) Tumors as Organs: Complex Tissues That Interface with the Entire Organism. *Developmental Cell*, **18**, 884-901. https://doi.org/10.1016/j.devcel.2010.05.012

[45] Kallinowski, F., Schlenger, K.H., Runkel, S., Kloes, M., Stohrer, M., Okunieff, P. and Vaupel, P. (1989) Blood Flow, Metabolism, Cellular Microenvironment, and Growth Rate of Human Tumor Xenografts. *Cancer Research*, **49**, 3759-3764.

[46] Guiot, C., Degiorgis, P.G, Delsanto, P.P., Gabriele, P. and Deisboeck, T.S. (2003) Does Tumor Growth Follow a "Universal Law"? *Journal of Theoretical Biology*, **225**, 147-151. https://doi.org/10.1016/S0022-5193(03)00221-2

[47] Moatemed, F., Sahimi, M. and Naeim, F. (1998) Fractal Dimension of the Bone Marrow in Metastatic Lesions. *Human Pathology*, **29**, 1299-1303. https://doi.org/10.1016/S0046-8177(98)90261-1

[48] West, G.B. and Brown, J.H. (2004) Life's Universal Scaling Laws. *Physics Today*, **57**, 36-44. https://doi.org/10.1063/1.1809090

[49] West, G.B., Brown, J.H. and Enquist, B.J. (2001) A General Model for Ontogenic Groth. *Nature*, **413**, 628-631. https://doi.org/10.1038/35098076

[50] Makarieva, A.M., Nefiodov, A.V. and Li, B.-L. (2020) Life's Energy and Information: Contrasting Evolution of Volume versus Surface-Specific Rates of Energy Consumption. *Entropy*, **22**, Article No. 1025. https://doi.org/10.3390/e22091025

[51] Baish, J.W. and Jain, R.K. (2000) Fractals and Cancer. *Cancer Research*, **60**, 3683-3688.

[52] Tubiana, M. (1989) Tumor Cell Proliferation Kinetics and Tumor Growth Rate. *Acta Oncologica*, **28**, 113-121. https://doi.org/10.3109/02841868909111193

[53] Gazit, Y. (1996) Fractal Vasculature and Vascular Network Growth Modeling in Normal and Tumor Tissue. PhD Thesis, Massachusetts Institute of Technology, Cambridge, MA.

[54] Sabo, E., Boltenko, A., Sova, Y., Stein, A., Kleinhaus, S. and Resnick, M.B. (2001) Microscopic Analysis and Significance of Vascular Architectural Complexity in Renal Cell Carcinoma. *Clinical Cancer Research*, **7**, 533-537.

[55] Herman, A.B., Savage, V.M. and West, G.B. (2011) A Quantitative Theory of Solid Tumor Growth, Metabolic Rate and Vascularization. *PLoS ONE*, **6**, e22973. https://doi.org/10.1371/journal.pone.0022973

[56] Bauer, W. and Mackenzie, C.D. (1995) Cancer Detection via Determination of Fractal Cell Dimension. arXiv:patt-sol/9506003.

[57] Mandelbrot, B.B. and Wheeler, J.A. (1983) The Fractal Geometry of Nature. *American Journal of Physics*, **51**, 286-287. https://doi.org/10.1119/1.13295

[58] Huang, W., Yen, R.T., McLaurine, M. and Bledsoe, G. (1996) Morphometry of the

Human Pulmonary Vasculature. *Journal of Applied Physiol*ogy, **81**, 2123-2133. https://doi.org/10.1152/jappl.1996.81.5.2123

[59] Savage, Van M., Gillooly, J.F., Woodruff, W.H., West, G.B., Allen, A.P., Enquist, B.J. and Brown, J.H. (2014) The Predominance of Quarter-Power Scaling in Biology. *Functional Ecology*, **18**, 257-282. https://doi.org/10.1111/j.0269-8463.2004.00856.x

[60] Szigeti, G.P., Szasz, O. and Hegyi, G. (2017) Connections between Warburg's and Szentgyorgyi's Approach about the Causes of Cancer. *Journal of Neoplasm*, **1**, 1-13.

[61] Voet, D., Voet, J.G. and Pratt, C.W. (2006) Fundamentals of Biochemistry. 2nd Edition, John Wiley and Sons, Inc., Hoboken, 547, 556.

[62] Pamatmat, M.M. (2005) Measuring Aerobic and Anaerobic Metabolism of Benthic Infauna under Natural Conditions. *Journal of Experimental Zoology*, **228**, 405-413. https://doi.org/10.1002/jez.1402280303

[63] Costello, L.C. and Franklin, R.B. (2006) Tumor Cell Metabolism: The Marriage of Molecular Genetics and Proteomics with Cellular Intermediary Metabolism; Proceed with Caution! *Molecular Cancer*, **5**, Aticle No. 59. https://doi.org/10.1186/1476-4598-5-59

[64] Warburg, O. (1956) On the Origin of Cancer Cells. *Science*, **123**, 309-314. https://doi.org/10.1126/science.123.3191.309

[65] Jeon, S.-M. and Hay, N. (2018) Expanding the Concepts of Cancer Metabolism. *Experimental & Molecular Medicine*, **50**, 1-3. https://doi.org/10.1038/s12276-018-0070-9

[66] Ward, P.S. and Thompson, C.B. (2012) Metabolic Reprogramming: A Cancer Hallmark Even Warburg Did Not Anticipate. *Cancer Cell*, **21**, 297-308. https://doi.org/10.1016/j.ccr.2012.02.014

[67] Hand, S.V. and Menze, M.A. (2008) Commentary Mitochondria in Energy-Limited States: Mechanisms That Blunt the Signaling of Cell Death. *The Journal of Experimental Biology*, **211**, 1829-1840. https://doi.org/10.1242/jeb.000299

[68] Szasz, O., Vincze, G., Szigeti, G.P., Benyo, Z. and Szasz, A. (2018) An Allometric Approach of Tumor-Angiogenesis. *Medical Hypotheses*, **116**, 74-78. https://doi.org/10.1016/j.mehy.2018.03.015

[69] Tannock, I.F. (1968) The Relation between Cell Proliferation and the Vascular System in a Transplanted Mouse Mammary Tumour. *British Journal of Cancer*, **22**, 258-273. https://doi.org/10.1038/bjc.1968.34

[70] Milotti, E., Vyshemirsky, V., Sega, M. and Chignola, R. (2012) Interplay between Distribution of Live Cells and Growth Dynamics of Solid Tumours. *Scientific Reports*, **2**, Article No. 990. https://doi.org/10.1038/srep00990

[71] Milotti, E., Vyshemirsky, V., Sega, M. and Chignola, R. (2013) Metabolic Scaling in Solid Tumours. *Scientific Reports*, **3**, Article No. 1938. https://doi.org/10.1038/srep01938

[72] Painter, P.R. (2005) Allometric Scaling of the Maximum Metabolic Rate of Mammals: Oxygen Transport from the Lungs to the Heart Is a Limiting Step. *Theoretical Biology and Medical Modelling*, **2**, Article No. 31. https://doi.org/10.1186/1742-4682-2-31

[73] Szasz, O. and Szigeti, Gy.P. (2020) Allometric Scaling by the Length of the Circulatory Network. *Frontiers in Physiology Fractal and Network Physiology*. (Under Review)

[74] Shim, E.B., Kim, Y.S. and Deisboeck, T.S. (2007) 2D FEM Tumor Angiogenesis Model 1 Analyzing the Dynamic Relationship between Tumor Growth and Angiogenesis in a Two Dimensional Finite Element Model. https://arxiv.org/ftp/q-bio/papers/0703/0703015.pdf

[75] Landini, G. and Rippin, J.W. (1993) Fractal Dimensions of the Epithelial-Connective Tissue Interfaces in Premalignant and Malignant Epithelial Lesions of the Floor of the Mouth. *Analytical and Quantitative Cytology and Histology*, **15**, 144-149.

[76] McDonald, M.D. and Choyke, P.L. (2003) Imaging of Angiogenesis from Microscope to Clinic. *Nature Medicine*, **9**, 713-725. https://doi.org/10.1038/nm0603-713

[77] Ichim, L. and Dobrescu, R. (2013) Characterization of Tumor Angiogenesis Using Fractal Measures. 19*th International Conference on Control Systems and Computer Science*, Bucharest, 29-31 May 2013, 345-349. https://doi.org/10.1109/CSCS.2013.18 https://www.researchgate.net/publication/261092279

[78] Jurczyszyn, K., Osiecka, B.J. and Ziołkowski, P. (2012) The Use of Fractal Dimension Analysis in Estimation of Blood Vessels Shape in Transplantable Mammary Adenocarcinoma inWistar Rats after Photodynamic Therapy Combined with Cysteine Protease Inhibitors. Computational and Mathematical Methods in Medicine, **2012**, Article ID: 793291. https://doi.org/10.1155/2012/793291

[79] Avakian, A., Kalina, R.E., Sage, E.H., Rambhia, A.H., Elliott, K.E., Chuang, E.L., Clark, J.I., Hwang, J.N. and Parsons-Wingerter, P. (200) Fractal Analysis of Region-Based Vascular Change in the Normal and Non-Proliferative Diabetic retina. *Current Eye Research*, **24**, 274-280. https://doi.org/10.1076/ceyr.24.4.274.8411

[80] Parsons-Wingerter, P., Chandrasekharan, U.M., McKay, T.L., Radhakrishnan, K., DiCorleto, P.E., Albarran, B. and Farr, A.G. (2006) A VEGF165-Induced Phenotypic Switch from Increased Vessel Density to Increased Vessel Diameter and Increased Endothelial NOS Activity. *Microvascular Research*, **72**, 91-100. https://doi.org/10.1016/j.mvr.2006.05.008

[81] Guidolin, D., Vacca, A., Nussdorfer, G.G. and Ribatti, D. (2004) A New Image Analysis Method Based on Topological and Fractal Parameters to Evaluate the Angiostatic Activity of Docetaxel by Using the Matrigel Assay *in Vitro*. *Microvascular Research*, **67**, 117-124. https://doi.org/10.1016/j.mvr.2003.11.002

[82] Mancardi, D., Varetto, G., Bucci, E., Maniero, F. and Guiot, C. (2008) Fractal Parameters and Vascular Networks: Facts & Artifacts. *Theoretical Biology and Medical Modelling*, **5**, Article No. 12. https://doi.org/10.1186/1742-4682-5-12

International Journal of Clinical Medicine, 2021, 12, 297-305
https://www.scirp.org/journal/ijcm
ISSN Online: 2158-2882
ISSN Print: 2158-284X

The Shift of the Ischial Region during Maneuvering the Standard Wheelchair and the Electric Wheelchair in Healthy Adults

Mikiko Uemura[1,2*], Masaharu Sugimoto[3], Ryoko Shimizu[4], Noriaki Maeshige[2], Yoshiyuki Yoshikawa[5], Hidemi Fujino[2]

[1]Faculty of Health Science, Department of Rehabilitation, Kansai University of Welfare Sciences, Kashiwara, Japan
[2]Department of Rehabilitation Science, Graduate School of Health Sciences, Kobe University, Kobe, Japan
[3]Toyama Rehabilitation Medical Health and Welfare College, Toyama, Japan
[4]Department of Rehabilitation, Kansai Medical University Hospital, Hirakata, Japan
[5]Faculty of Health Sciences, Department of Rehabilitation, Naragakuen University, Nara, Japan
Email: *uemura@tamateyama.ac.jp

How to cite this paper: Uemura, M., Sugimoto, M., Shimizu, R., Maeshige, N., Yoshikawa, Y. and Fujino, H. (2021) The Shift of the Ischial Region during Maneuvering the Standard Wheelchair and the Electric Wheelchair in Healthy Adults. *International Journal of Clinical Medicine*, **12**, 297-305.
https://doi.org/10.4236/ijcm.2021.127026

Received: June 28, 2021
Accepted: July 23, 2021
Published: July 26, 2021

Abstract

Pressure injuries are frequent secondary complications that occur in patients with Spinal Cord Injury (SCI), and the recurrence rate of ischial pressure injury is highest in SCI patients. Most SCI patients use wheelchairs, and some studies have shown a relationship between buttock pressure and sitting posture. However, the pressure distribution during wheelchair maneuvering is unclear. We measured and compared the shift of the ischial region when maneuvering a standard wheelchair or electric wheelchair in healthy adults. The subjects drove wheelchairs on a flat ground of 10 m and the shift of ischial region was measured with a pressure distribution-measuring device. The ischial region shifted forward or backward while maneuvering both the standard wheelchair and the electric wheelchair, and the shift rate of the ischial region was not significantly different between the standard wheelchair and the electric wheelchair. The ischial region shift occurred when the forward head moved by the video while maneuvering both a standard wheelchair and an electric wheelchair. Therefore, the shift might occurred because the pelvis shifted forward in conjunction with head movement during maneuvering of both the standard wheelchair and the electric wheelchair. This result showed that it is important to reduce head and trunk movements when maneuvering a wheelchair to reduce the shear force on the buttocks and prevent pressure injuries.

Keywords

Spinal Cord Injury, Pressure Ulcer, Wheelchair, Buttock Pressure

1. Introduction

Pressure injuries are caused by pressure and shear forces. The activity level of Spinal Cord Injury (SCI) patients who maneuver a wheelchair by themselves is high, and they can drive a car, carry out work, etc. [1]. SCI patients have pathologically protruding bone due to muscle atrophy of the buttocks and joint contracture, which are risk factors for pressure injury development [2]. Pressure injury frequently occurs particularly on the sacral area, ischial area, and the heel in SCI patients [3], and the postoperative recurrence rate was 27% [4]. Moreover, Jensen reported that the recurrence rate of ischial pressure injury was highest at 53% compared to that of the other site [5]. The ischial pressure injury often undergoes flap surgery but this surgical treatment needs 2 weeks-bed rest [6], and bed rest induces disuse syndrome such as autonomic disorder and muscle atrophy. Thus, it is crucial to prevent ischial pressure injury development and recurrence. Therefore, some studies have compared the seating pressure distribution effects of seating cushions [7] [8] and the effects of back support and the reclining wheelchair angle on buttock pressure [9] [10] [11] to prevent ischial and sacral pressure injuries. However, these studies assessed buttock pressure in a sedentary sitting posture, and the pressure distribution during wheelchair maneuvering is unclear. As mentioned above, pressure and shear forces cause pressure injuries. The shear force and pressure may occur on the ischial area when the wheelchair cause maneuvers because the trunk and pelvis move during maneuvering.

Therefore, we revealed the shear stress on the ischial site while maneuvering the standard type of wheelchair and electric wheelchair.

2. Subjects and Methods

The subjects were 20 healthy adults (10 men and 10 women). Height, weight, Body Mass Index (BMI), and upper limb length were measured. Those with a BMI of 25 kg/m^2 or more were excluded, and 19 subjects (10 males and 9 females) were measured, and all subjects were right-handed.

The change in the maximum pressure section during maneuvering of the wheelchair was measured. A pressure distribution-measuring device (FSA; Force Sensitive Applications, Takano, Japan) was used to measure the sitting pressure. It consists of a 533 mm^2, pressure measure seat including 16 × 16 pressure sensor (1 piece 25.4 mm, center spacing 3.1 mm), data conversion interface module, wireless kit, and Personal Computer (PC). A standard wheelchair was used as a self-propelled wheelchair in the experiment. The electric wheelchair used was JW Active (Yamaha Motor, Japan). Two standard wheelchairs of different seat widths were used according to the physique of the subject. An electric wheelchair joystick was installed on the right armrest. The footrest for both self-propelled and electric was adjusted so that the height of the footrest was 5 cm or more from the floor. The FSA seat was laid along the front edge of the wheelchair seat. The FSA sampling interval was set at 5 Hz. The subjects wore seamless shorts. In this ex-

periment, to clarify the position of the ischial region, aluminum plates with a length of 4 cm and a width of 2 cm were attached to both sciatic regions of the subject, and a dressing material (Tegasorb™ hydrocolloid dressing, 3M Healthcare) was attached for sensor protection. This was confirmed by using a friction reduction tool (multi-glove, paramount bed) to determine whether there was any discrepancy between the actual position of the ischial region and the position displayed using the device.

For the driving method, a certain method was set so that there would be no difference due to driving. For self-propelled wheelchairs, the apex of the hand rim was set to 0˚. Instructions were given to drive in the range of 30˚ to 60˚ forward, and the number of drives was set to once per second according to the metronome. The electric wheelchair was set to 3.8 km/h and the subjects were instructed to move only their right hand. After practicing the driving method for both the standard wheelchair and the electric wheelchair, the pressure on the ischial region was measured by driving on a flat ground of 10 m three times each. The movement of the body during driving was recorded from the side using a PC equipped with a camera.

A chi-square test was used for statistical analysis, and the risk rate was set to less than 5% in each case.

3. Results

The characteristics of the participants are listed in Table 1. The average driving time of a self-propelled wheelchair was 10.1 ± 1.4 seconds for men and 10.7 ± 2.1 seconds for women, the average number of driving times was 10.0 ± 1.3 times for men and 10.6 ± 2.0 times for women, and the average driving speed was 3.63 ± 0.51 m/s for men and 3.50 ± 0.62 m/s for women. Regarding the presence or absence of ischial displacement, it was judged that the ischial displacement occurred only when the maximum pressure region of the ischial pressure distribution moved anteriorly or posteriorly, and the position of the original maximum pressure region moved in the same direction. The displacement of the ischial region that occurred in this study was a forward sensor. Figure 1 shows an example in which the sitting pressure distribution in the ischial region changed and displacement occurred when driving a self-propelled wheelchair. Figure 1(a) shows the distribution at the moment when the hand rim is pushed forward, Figure 1(b) shows the distribution at the moment when the hand is released from the hand rim, and Figure 1(c) shows the distribution at the moment when the hand rim is gripped again. The area surrounded by a square on the sensor seat was the position of the ischium. A comparison of Figure 1(a) and Figure 1(b) shows that the maximum pressure region of both ischia moves forward, and when comparing Figure 1(b) and Figure 1(c), the maximum pressure region returns to the rear.

For electric wheelchairs, the moment of the joystick was pushed forward was set as the start of driving. Similar to the self-propelled wheelchair, those who

showed a change in the maximum pressure region during driving were taken as an example of displacement in the ischial region. In self-propelled wheelchairs, the number of people with ischial displacement was eight for men and three for women, and the displacement detection rates (number of detectors/subjects) were 80% for men and 33.3% for women. In electric wheelchairs, the number of people with ischial displacement was three for men and three for women, and the displacement detection rates were 30% for men and 33.3% for women. Table 2 and Table 3 show the number of deviation section for each subject, Table 4 shows the number of people who have a deviation in each wheelchair.

No significant association was found in the ischial displacement between the wheelchairs in all subjects. Distinguishing between men and women, a significant association was found between self-propelled wheelchair driving and ischial displacement in men ($p < 0.05$), while no significant association was found in women.

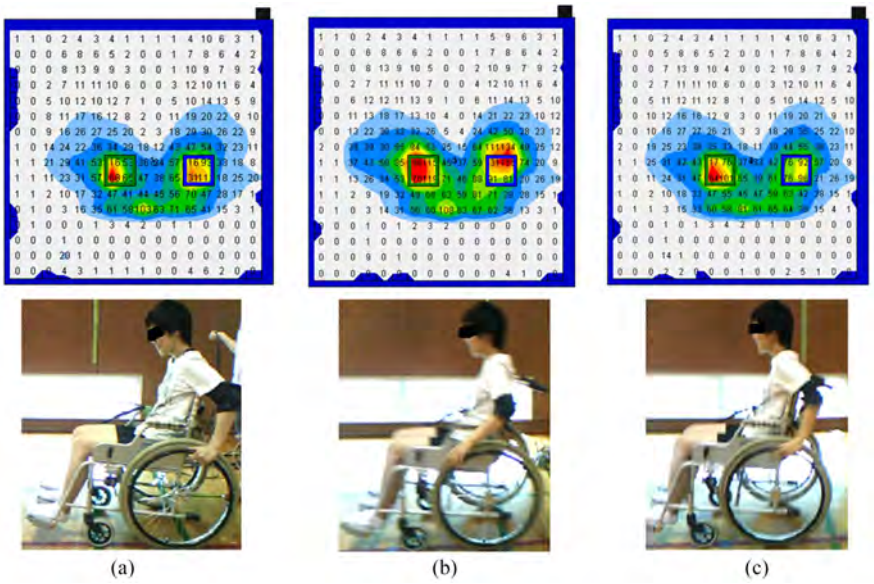

Figure 1. Sitting pressure distribution in the ischial region. The area surrounded by qualifications means ischial area. (a): The moment that a subject pushed the hand rim forward; (b): The moment that a subject released the hand rim; (c): The moment that a subject griped the hand rim again. Right and left ischial area shifted forward when a subject released the hand rim (a, b), and the ischial are returned the rear (b, c).

Table 1. Characteristics of subjects.

	Male	Female
Age (years)	22 ± 1.9	21 ± 0.8
Height (cm)	169.2 ± 3.92	160.1 ± 5.17
Wight (kg)	58.2 ± 4.42	53.4 ± 5.66
BMI (kg/m^2)	20.3 ± 1.27	20.3 ± 1.38
Upper limb length (cm)	55.5 ± 1.43	51.8 ± 2.15

Table 2. The number of deviation section in male.

	Standard wheelchair 1st drive		Standard wheelchair 2nd drive		Standard wheelchair 3rd drive		Electric wheelchair 1st drive		Electric wheelchair 2nd drive		Electric wheelchair 3rd drive	
Ischial	Left	Right	Left	Right	Left	Right	Left	Right	Left	Right	Left	Right
Case A	1	1	0	1	0	1	0	0	0	0	0	0
Case B	1	1	0	1	0	1	0	0	0	0	0	0
Case C	0	1	1	1	0	0	0	0	0	0	1	1
Case D	0	0	1	1	1	1	1	1	0	0	1	1
Case E	0	0	0	0	0	0	0	0	0	0	0	0
Case F	1	1	0	0	0	0	0	0	0	0	0	0
Case G	0	0	0	0	1	0	0	0	0	0	1	0
Case H	0	0	1	0	0	0	0	0	0	0	0	0
Case I	1	1	0	1	1	1	0	0	0	0	0	0
Case J	0	0	0	0	0	0	0	0	0	0	0	0

Table 3. The number of deviation section in female.

	Standard wheelchair 1st drive		Standard wheelchair 2nd drive		Standard wheelchair 3rd drive		Electric wheelchair 1st drive		Electric wheelchair 2nd drive		Electric wheelchair 3rd drive	
Ischial	Left	Right	Left	Right	Left	Right	Left	Right	Left	Right	Left	Right
Case a	0	0	0	0	0	0	0	0	0	0	0	0
Case b	0	0	0	0	0	0	0	0	1	0	0	0
Case c	0	0	0	0	1	0	1	0	0	0	1	1
Case d	1	0	1	0	1	0	0	0	0	0	0	0
Case e	0	0	0	0	0	0	0	0	0	0	0	0
Case f	0	0	0	0	0	0	0	0	0	0	0	0
Case g	1	1	1	1	0	0	1	1	0	0	0	0
Case h	0	0	0	0	0	0	0	0	0	0	0	0
Case i	0	0	0	0	0	0	0	0	0	0	0	0
Case j	0	0	0	0	0	0	0	0	0	0	0	0

Table 4. The number of people who have a deviation in each wheelchair.

	Deviation (+)	Deviation (−)
Satndard wheelchair	11 (8, 3)	8 (2, 6)
Electric wheelchair	6 (3, 3)	13 (7, 6)

Number (male, female).

4. Discussion

This study showed that the pressure of the ischial region shifted during maneuvering of the wheelchair. It is considered that the change in the position of the maximum pressure region during wheelchair driving, which occurred in this

study, reflects the anterior-posterior movement of the ischium on the seat. This movement of the ischium is thought to be caused by the anterior-posterior tilt of the trunk that occurs during driving and the accompanying anterior-posterior tilt of the pelvis. When the ischium moves on the seat due to the anterior-posterior tilt of the pelvis, a shift occurs between the ischium and the subcutaneous tissue, which is considered to be a risk factor for the development of pressure ulcers. Therefore, we provide guidance on wheelchair prescriptions and contraindications for patients with SCI who have pressure ulcers in the ischial region and patients who require pressure ulcer management in the ischial region by measuring the displacement of the ischial region when driving a wheelchair in a healthy person. Based on this, we compared the changes in the maximum pressure of the ischial region when driving two types of wheelchairs, a self-propelled wheelchair, and an electric wheelchair, and investigated the factors that cause the deviation.

No significant association was found between the wheelchair and ischial region in any of the subjects. In contrast, a significant association was observed in men. Those who were found to have a displacement of the ischial region tended to have pronounced head movements while driving based on the observation results of the video. In addition, because all changes in the maximum pressure region occur anteriorly, the pelvis is considered to tilt backward and the ischium moves anteriorly. However, according to Yang's study [12] at a rate of 0.9 m/s, there is little activity in the core muscles, and when driving on flat ground, there is almost no activity of the lower limb muscles, and there is no anterior-posterior tilt of the trunk [13]. In this study, the average driving speed of men is 1.01 ± 0.14 m/s, and women 0.97 ± 0.17 m/s, which is equivalent to the result of Yang's study [13], so it is unlikely that muscle contraction caused movement in the pelvis.

The upper limb forms of self-propelled wheelchairs are classified into four types [14], and all of them apply force diagonally forward when driving [15]. A force was applied in the vertical direction and backward from the hand rim according to the law of action and reaction (**Figure 2**). The ischial region might shift as the upper limbs receive this backward force and the pelvic tilt backward.

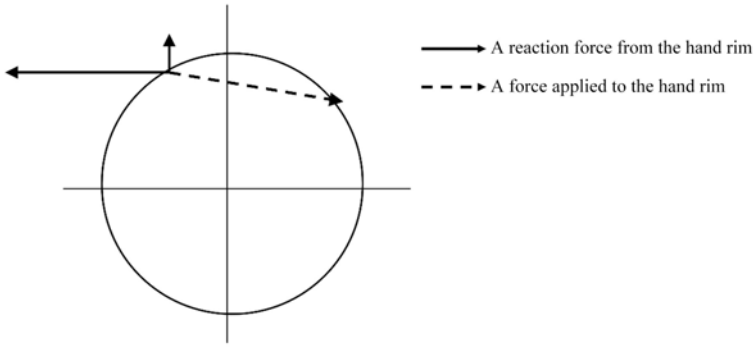

Figure 2. The force applied on the hand rim. A force was applied in the vertical direction and backward from the hand rim during wheelchair maneuvering.

There was also an example in which a change in the maximum pressure was observed while measuring with an electric wheelchair. The change in the maximum pressure was observed only when the joystick was pushed forward at the start of driving. Because the maximum pressure region did not change during driving, it is possible that when the joystick was pushed forward, the subject's head was bent forward and the trunk was tilted back and forth, causing a shift. Therefore, concerning driving an electric wheelchair on a straight line on flat ground as measured this time, it is unlikely that the ischial region will shift unless the head and trunk are moved when pushing the joystick forward.

The results of this study suggest that the movement of the head and trunk during driving may cause a shift in the ischial region. Therefore, it is desirable to prescribe an electric wheelchair to the patient or instruct the patient to drive with minimal movement of the head and trunk. For patients with SCI who are self-propelled in a wheelchair as a means of transportation, restricted activity due to pressure ulcers in the ischial region leads to a decrease in Quality of Life (QOL) [16]. To improve the QOL of SCI patients, it is desirable to use an electric wheelchair while the pressure ulcer in the ischial region is healing, and to teach them how to drive a self-propelled wheelchair from a preventive point of view after healing.

This study was conducted on flat ground under conditions in which the driving method was restricted. As the driving speed increases, the activity of the trunk muscles and the forward tilt of the trunk also increase [8]; therefore, it is predicted that the displacement of the ischial region will be larger than the result of this study if the driving speed is increased. As described above, it is necessary to assume driving in all situations to spend time in a wheelchair in daily life. By measuring the displacement of the ischial region under various conditions, such as gradient, speed, and activities of daily living, more advanced knowledge can be obtained. Therefore, measurement under different conditions, as described above, is an issue that should be examined in the future.

The FSA sensor mat used this time has a structure in which square sensors with a side of 25.4 mm are lined up at intervals of 3.1 mm. Because the sitting pressure is displayed only when it is applied to the sensor, the pressure applied between the sensors cannot be measured. Regardless of size, displacement is a risk factor for pressure ulcers; therefore, it is necessary to measure small changes in sitting pressure. However, because of the structure of the sensor mat used this time, it was only possible to measure the deviation in units of at least one square (25.4 mm + 3.1 mm^2). To investigate the displacement of the ischial region in more detail, it is necessary to re-verify it using a device that measures the displacement.

5. Conclusion

The ischial region shifted during the maneuvering of both the standard wheelchair and the electric wheelchair. Since it is thought that the movement of the

spinal column and trunk causes displacement, it is better not to use a self-propelled wheelchair during the period when protection of ischial pressure ulcers is required, such as in the early postoperative period. In addition, it is necessary to provide wheelchair users with guidance on driving methods that reduce the disengagement force.

Ethics

The purpose of the study was to explain to the subjects, and patient consent was obtained. All procedures were performed according to the principles of the Declaration of Helsinki.

Conflicts of Interest

The authors declare no conflicts of interest regarding the publication of this paper.

References

[1] Morita, T., Yamada, T., Watanabe, T. and Nagahori. E. (2015) Lifestyle Risk Factors for Pressure Ulcers in Community-Based Patients with Spinal Cord Injuries in Japan. *Spial Cord*, **53**, 476-481. https://doi.org/10.1038/sc.2015.18

[2] Verschueren, J.H.M., Post, M.W.M., de Groot, S., van der Woude, L.H.V., van Asbeck, F.W.A. and Rol, M. (2011) Occurrence and Predictors of Pressure Ulcers during Primary In-Patient Spinal Cord Injury Rehabilitation. *Spial Cord*, **49**, 106-112. https://doi.org/10.1038/sc.2010.66

[3] Flett H.M., Delparte J.J., Scovil C.Y., Higgins J., Laramee M.T. and Burns A.S. (2019) Determining Pressure Injury Risk on Admission to Inpatient Spinal Cord Injury Rehabilitation: A Comparison of the FIM, Spinal Cord Injury Pressure Ulcer Scale, and Braden Scale. *Archives of Physical Medicine and Rehabilitation*, **100**, 1881-1887. https://doi.org/10.1016/j.apmr.2019.04.004

[4] Ljung, A.C., Stenius, M.C., Bjelak, S. and Lagergren, J.F. (2017) Surgery for Pressure Ulcers in Spinal Cord-Injured Patients following a Structured Treatment Programme: A 10-Year Follow-Up. *International Wound Journal*, **14**, 355-359. https://doi.org/10.1111/iwj.12609

[5] Bates-Jensen, B.M., Guihan, M., Garber, S.L., Chin, A.S. and Burns, S.P. (2009) Characteristics of Recurrent Pressure Ulcers in Veterans with Spinal Cord Injury. *The Journal of Spinal Cord Medicine*, **32**, 34-42. https://doi.org/10.1080/10790268.2009.11760750

[6] Ishikawa, S. and Ichioka, S. (2019) Surgical Treatment of Pressure Ulcers. *Japan Society of Pressure Ulcers*, **21**, 18-23. (In Japanese)

[7] Mendes, P.V.B., Gradim, L.C.C., Silva, N.S., Allegretti, A.L.C., Carrijo, D.C.M. and da Cruz, D.M.C. (2019) Pressure Distribution Analysis in Three Wheelchairs Cushions of Subjects with Spinal Cord Injury. *Disability and Rehabilitation*: *Assistive Technology*, **14**, 555-560. https://doi.org/10.1080/17483107.2018.1463399

[8] Trewartha, M. and Stiller, K. (2011) Comparison of the Pressure Redistribution Qualities of Two Air-Filled Wheelchair Cushions for People with Spinal Cord Injuries. *Australian Occupational Therapy Journal*, **58**, 287-292. https://doi.org/10.1111/j.1440-1630.2011.00932.x

[9] Kobara, K., Osaka, H., Takahashi, H., Ito, T., Fujita, D. and Watanabe, S. (2015) In-

fluence of Rotational Axis Height of Back Support on Horizontal Force Applied to Buttocks in a Reclining Wheelchair. *Prosthetics and Orthotics International*, **39**, 397-404. https://doi.org/10.1177/0309364614543547

[10] Park, U.J. and Jang, S.H. (2011) The Influence of Backrest Inclination on Buttock Pressure. *Annals of Rehabilitation Medicine*, **35**, 897-906. https://doi.org/10.5535/arm.2011.35.6.897

[11] Zemp, R., Rhiner, J., Pluss, S., Togni, R., Plock, J.A. and Taylor, W.R. (2019) Wheelchair Tilt-in-Space and Recline Functions: Influence on Sitting Interface Pressure and Ischial Blood Flow in an Elderly Population. *BioMed Research International*, **2019**, Article ID: 4027976. https://doi.org/10.1155/2019/4027976

[12] Yang, Y.S., Koontz, A.M., Triolo, R.J., Mercer, J.L. and Boninger, M.L. (2006) Surface Electromyography Activity of Trunk Muscles during Wheelchair Propulsion. *Clinical Biomechanics*, **21**, 1032-1041. https://doi.org/10.1016/j.clinbiomech.2006.07.006

[13] Howarth, S.J., Polgar, J.M., Dickerson, C.R. and Callaghan, J.P. (2010) Trunk Muscle Activity during Wheelchair Ramp Ascent and the Influence of a Geared Wheel on the Demands of Postural Control. *Archives of Physical Medicine and Rehabilitation*, **91**, 436-442. https://doi.org/10.1016/j.apmr.2009.10.016

[14] Boninger, M.L., Souza, A.L., Copper, R.A., Fitzgerald, S.G., Koonts, A.M. and Fay, B.T. (2002) Propulsion Patterns and Pushrim Biomechanics in Manual Wheelchair Propulsion. *Archives of Physical Medicine and Rehabilitation*, **83**, 718-723. https://doi.org/10.1053/apmr.2002.32455

[15] Newsam, C.J., Rao, S.S. and Mulroy, S.J. (1999) Three Dimension Upper Extremity Motion during Manual Wheelchair Propulsion in Men with Different Levels of Spinal Cord Injury. *Gait and Posture*, **10**, 223-232. https://doi.org/10.1016/S0966-6362(99)00034-X

[16] Charlifue, S., Lammertse, D.P. and Adkins, R.H. (2004) Aging with Spinal Cord Injury: Changes in Selected Health Indices and Life Satisfaction. *Archives of Physical Medicine and Rehabilitation*, **85**, 1848-1853. https://doi.org/10.1016/j.apmr.2004.03.017

Call for Papers

International Journal of Clinical Medicine

ISSN: 2158-284X (Print) ISSN: 2158-2882 (Online)
https://www.scirp.org/journal/ijcm

International Journal of Clinical Medicine (IJCM) is a peer reviewed journal dedicated to the latest advancement of clinical medicine. The goal of this journal is to keep a record of the state-of-the-art research and to promote study, research and improvement within its various specialties.

Subject Coverage

The journal publishes original papers including but not limited to the following fields:

- Allergy and Clinical Immunology
- Cancer Research and Clinical Oncology
- Clinical Anaesthesiology
- Clinical Anatomy
- Clinical and Applied Thrombosis/Hemostasis
- Clinical and Experimental Allergy
- Clinical and Experimental Dermatology
- Clinical and Experimental Hypertension
- Clinical and Experimental Immunology
- Clinical and Experimental Medicine
- Clinical and Experimental Metastasis
- Clinical and Experimental Nephrology
- Clinical and Experimental Ophthalmology
- Clinical and Experimental Optometry
- Clinical and Experimental Otorhinolaryngology
- Clinical and Experimental Pathology
- Clinical and Experimental Pharmacology and Physiology
- Clinical and Molecular Allergy
- Clinical and Translational Oncology
- Clinical Anesthesia
- Clinical Apheresis
- Clinical Autonomic Research
- Clinical Biochemistry and Nutrition
- Clinical Biomechanics
- Clinical Cardiology
- Clinical Case Studies
- Clinical Child Psychology and Psychiatry
- Clinical Chiropractic
- Clinical Densitometry
- Clinical Effectiveness in Nursing
- Clinical Endocrinology and Metabolism
- Clinical Epidemiology
- Clinical Forensic Medicine
- Clinical Gastroenterology and Hepatology
- Clinical Genetics
- Clinical Haematology
- Clinical Hypertension
- Clinical Imaging
- Clinical Immunology
- Clinical Implant Dentistry and Related Research
- Clinical Interventions in Aging
- Clinical Laboratory Analysis
- Clinical Linguistics & Phonetics
- Clinical Lipidology
- Clinical Microbiology and Antimicrobials
- Clinical Microbiology and Infection
- Clinical Microbiology and Infectious Diseases
- Clinical Molecular Pathology
- Clinical Monitoring and Computing
- Clinical Neurology and Neurosurgery
- Clinical Neurophysiology
- Clinical Neuropsychology
- Clinical Neuroradiology
- Clinical Neuroscience
- Clinical Nursing
- Clinical Nutrition
- Clinical Obstetrics and Gynaecology
- Clinical Oncology and Cancer Research
- Clinical Ophthalmology
- Clinical Oral Implants Research
- Clinical Oral Investigations
- Clinical Orthopaedics and Related Research
- Clinical Otolaryngology
- Clinical Pathology
- Clinical Pediatric Emergency Medicine
- Clinical Periodontology
- Clinical Pharmacology & Toxicology
- Clinical Pharmacy and Therapeutics
- Clinical Physiology and Functional Imaging
- Clinical Practice and Epidemiology in Mental Health
- Clinical Psychology and Psychotherapy
- Clinical Psychology in Medical Settings
- Clinical Radiology
- Clinical Rehabilitation
- Clinical Research and Regulatory Affairs
- Clinical Research in Cardiology
- Clinical Respiratory
- Clinical Rheumatology
- Clinical Simulation in Nursing
- Clinical Sleep Medicine
- Clinical Techniques in Small Animal Practice
- Clinical Therapeutics
- Clinical Toxicology
- Clinical Transplantation
- Clinical Trials
- Clinical Ultrasound
- Clinical Virology
- Complementary Therapies in Clinical Practice
- Consulting and Clinical Psychology
- Contemporary Clinical Trials
- Controlled Clinical Trials
- Diabetes Research and Clinical Practice
- Evaluation in Clinical Practice
- Fundamental & Clinical Pharmacology
- Hereditary Cancer in Clinical Practice
- Human Psychopharmacology: Clinical and Experimental
- Innovations in Clinical Neuroscience
- Laboratory and Clinical Medicine
- Neurophysiologie Clinique/Clinical Neurophysiology
- Nutrition in Clinical Practice
- Pacing and Clinical Electrophysiology
- Psychiatry in Clinical Practice
- Therapeutics and Clinical Risk Management
- Veterinary Clinical Pathology

We are also interested in short papers (letters) that clearly address a specific problem, and short survey or position papers that sketch the results or problems on a specific topic. Authors of selected short papers would be invited to write a regular paper on the same topic for future issues of the ***IJCM***.

Notes for Intending Authors

All manuscripts submitted to IJCM must be previously unpublished and may not be considered for publication elsewhere at any time during IJCM's review period. Paper submission will be handled electronically through the website. All papers are refereed through a peer review process. Additionally, accepted ones will immediately appear online followed by printed in hard copy. For more details about the submissions, please access the website.

Website and E-Mail

https://www.scirp.org/journal/ijcm Email: ijcm@scirp.org

What is SCIRP?

Scientific Research Publishing (SCIRP) is one of the largest Open Access journal publishers. It is currently publishing more than 200 open access, online, peer-reviewed journals covering a wide range of academic disciplines. SCIRP serves the worldwide academic communities and contributes to the progress and application of science with its publication.

What is Open Access?

All original research papers published by SCIRP are made freely and permanently accessible online immediately upon publication. To be able to provide open access journals, SCIRP defrays operation costs from authors and subscription charges only for its printed version. Open access publishing allows an immediate, worldwide, barrier-free, open access to the full text of research papers, which is in the best interests of the scientific community.

- High visibility for maximum global exposure with open access publishing model
- Rigorous peer review of research papers
- Prompt faster publication with less cost
- Guaranteed targeted, multidisciplinary audience

Scientific Research Publishing

Website: https://www.scirp.org

Subscription: sub@scirp.org

Advertisement: service@scirp.org